Theory of photothermal wave diffraction tomography via spatial Laplace spectral decomposition

1991 J. Phys. A: Math. Gen. 24 2485

(http://iopscience.iop.org/0305-4470/24/11/016)

J. Phys. A: Math. Gen. 24 (1991) 2485-2505. Printed in the UK

Theory of photothermal wave diffraction tomography via spatial Laplace spectral decomposition

Andreas Mandelis

Photoacoustic and Photothermal Sciences Laboratory, Department of Mechanical Engineering and Ontario Laser and Lightwave Research Center, University of Toronto, Toronto, Canada M5S 1A4

Received 4 October 1990

Abstract. Laser-generated thermal wave diffraction theory is presented as a perturbative Born (or Rytov) approximation in a two-dimensional spatial domain for use with tomographic image reconstruction methodologies. The ranges of validity of the pertinent two-dimensional spatial-frequency/thermal wavenumber domain complex plane contours are investigated in terms of the existence of inverse spatial Laplace transforms in the mean-square sense. The spectral decomposition of the Laplace transforms according to a Laplace diffraction theorem is shown to involve regular complex-valued propagation functions, which represent the two-dimensional Laplace transform of a scattering object along semicircular arcs comprising the object's thermal wavenumber domain. A discussion of the complex thermal-wave spatial frequency domain content is also presented, with a view to tomographic recovery of the scattering object field.

1. Introduction

The use of optically excited thermal waves in condensed phase materials as probes of subsurface features or defects has dramatically increased in recent years [1]. Most applications to imaging typically involve two-dimensional scanning with a laser beam, and photothermal detection of projection images by a spatially integrating sensor, such as a piezoelectric transducer [2] or a pyroelectric transducer [3] placed below the sample under investigation. Other popular schemes involve local recording of projectional photothermal images including microphonic photoacoustic microscopy [4] and photothermal beam deflection imaging [5]. Total (or partial) spatial integration of the thermal-wave field is to be understood as a surface integral limited either by the active detector area (the case of back-surface piezoelectric or pyroelectric detection), or by the magnitude of the thermal diffusion length in the neighbourhood of the optically excited surface (the case of microphonic detection [6]). Spatial integration may further take the form of a line integral, such as the case of photothermal beam deflection, or Mirage effect, imaging along the length of the intersection between a broad pump source and a probe laser beam. All the above photothermal scanning and detection modes using a single exciting laser beam are incapable of providing depth imaging of sample cross-sections involving the subsurface location of defects. More sophisticated imaging methods based on thermal-wave interference from two coherently [7, 8] or anticoherently intensity-modulated laser beams have succeeded in providing estimates of the depth of a defect/scatterer. These methods depend on the resolution of an infrared blackbody radiometric emission detector [7], or a thin metallic pin capacitively

0305-4470/91/112485+21$03.50

coupled to a pyroelectric detector [9], to measure the local value of the thermal-wave field across the back-surface of a sample, i.e. in the transmission mode. A photothermal method based on the Mirage effect has been utilized to obtain depth information on the presence of defects by means of a tomographic-like procedure [10], limited by the line-integral nature of the probe laser beam to point-by-point reconstruction of projectional images upon correlation of angular scans. This technique, however, cannot yield proper tomographic imaging of cross-sectional planes in materials, due to the line-integral nature of the probe beam. Recently, a new tomographic method, based on the detection of thermal waves by a thin-film pyroelectric detector [9] has been utilized to generate cross-sectional thermal-wave tomograms for the first time [11]. Reconstructions of material cross-sections were obtained based on modification of algorithms, which were originally developed for X-ray tomograms. Such ray-like treatment of the highly dispersive, diffusive thermal-wave field can only be used as a crude approximation; it was made apparent immediately [11] that, because of diffraction (and, perhaps, refraction), more accurate models of the thermal-wave propagation had to be considered in order to achieve undistorted reconstructions and improved spatial resolution. There have been several theoretical models of thermal-wave propagation, based on wave mechanics in three dimensions in homogeneous [12, 13] and anisotropic [14] media. For the consideration of the tomographic theory in the present work, it was found most convenient to treat the photothermal wave propagation in terms of a spatial Laplace transform diffractive formalism derived from the highly damped nature of these pseudowaves [15].

In this paper we present the theoretical basis for photothermal wave diffraction tomography in the limit of a perturbative first Born (or Rytov) approximation for laterally translationally invariant solids and defects in solids. Unlike the standard spatial Fourier transform approach familiar from optical image analysis [16], careful consideration of the parameter range and convergence of inversion integrals along appropriate contours associated with the complex spatial Laplace domain variables must be given. The pivotal role of the Dirac delta function as a closure relation towards obtaining analytical bounded inversions in the complex thermal-wave spatial frequency domain and its interpretation in terms of Cauchy principal value integral forms is investigated in formulating the forward propagation field problem. Spectral decomposition of the Laplace variables in the complex plane of spatial frequencies is shown to lead to a Laplace diffraction theorem and spectral coverage criteria akin to those found in ultrasonic tomography [17].

2. Green's function formulation of the forward thermal-wave diffractive tomographic problem

On harmonic optical excitation of the boundary S enclosing some inhomogeneous region in space, R, and having the functional form

$$I(\boldsymbol{r}, t) = I_0(\boldsymbol{r}) \exp(-\mathrm{i}\omega t) \tag{1}$$

where I is the incident optical irradiance on S and $\omega = 2\pi f$ is the optical beam intensity modulation angular frequency, the resulting photothermal wavefield in R can be described fully by the equation [18]

$$\nabla K(\boldsymbol{r}) \cdot \nabla T(\boldsymbol{r}) + K(\boldsymbol{r}) \nabla^2 T(\boldsymbol{r}) + \mathrm{i}\omega \rho(\boldsymbol{r}) c(\boldsymbol{r}) T(\boldsymbol{r}) = 0 \tag{2}$$

where $T(\boldsymbol{r})$ is the spatial part of the modulated temperature field,

$$\Theta(\boldsymbol{r}, t) = T(\boldsymbol{r}) \exp(-i\omega t) \tag{3}$$

and $K(\boldsymbol{r})$, $\rho(\boldsymbol{r})$, $c(\boldsymbol{r})$ are the coordinate-dependent thermal conductivity, density and specific heat of the matter in R at location $\boldsymbol{r}$ from a suitably chosen origin. Equation (2) may be written in the form

$$\nabla^2 T(\boldsymbol{r}) + i\left(\frac{\omega}{\alpha(\boldsymbol{r})}\right) = -\left(\frac{\nabla K(\boldsymbol{r})}{K(\boldsymbol{r})}\right) \cdot \nabla T(\boldsymbol{r}) \tag{4}$$

where

$$\alpha(\boldsymbol{r}) \equiv K(\boldsymbol{r})/\rho(\boldsymbol{r})c(\boldsymbol{r}) \tag{5}$$

is the local thermal diffusivity. In the case where the thermal conductivity of the matter in R does not vary drastically with position, so that the fractional change of $K(\boldsymbol{r})$ in one local thermal wavelength (see below) is small, the right-hand-side of equation (4) may be neglected, which then yields the Helmholtz pseudowave equation [15]

$$(\nabla^2 + \tilde{k}^2(\boldsymbol{r}))\, T(\boldsymbol{r}) = 0. \tag{6}$$

In equation (6) $\tilde{k}(\boldsymbol{r})$ is the complex thermal wavenumber given by

$$\tilde{k}(\boldsymbol{r}; \omega) = (1+i)(\omega/2\alpha(\boldsymbol{r}))^{1/2} \equiv k(\boldsymbol{r}; \omega)\, e^{i\pi/4} \tag{7}$$

with the local thermal wavelength defined as

$$\lambda_t(\boldsymbol{r}; \omega) = 2\pi(\alpha(\boldsymbol{r})/\omega)^{1/2}. \tag{8}$$

In what follows all quantities bearing a tilde are understood to have the complex dependence designated in equation (7), i.e. equal real and imaginary components in the first quadrant of the relevant variable.

Letting the thermal diffusivity of the (assumed homogeneous) medium surrounding the object region R be α_0, equation (6) may be replaced by a modified Helmholtz pseudowave equation:

$$(\nabla^2 + \tilde{k}_0^2)\, T(\boldsymbol{r}) = -F(\boldsymbol{r})\, T(\boldsymbol{r}) \tag{9}$$

where

$$F(\boldsymbol{r}) = \begin{cases} \tilde{k}_0^2(n^2(\boldsymbol{r}) - 1) & \boldsymbol{r} \in R \\ 0 & \boldsymbol{r} \notin R \end{cases} \tag{10}$$

and

$$\tilde{k}_0 = (1+i)(\omega/2\alpha_0)^{1/2} \equiv k_0\, e^{i\pi/4} \tag{11}$$

and

$$n(\boldsymbol{r}) \equiv (\alpha_0/\alpha(\boldsymbol{r}))^{1/2}. \tag{12}$$

$n(\boldsymbol{r})$ is a measure of the variation of the values of the thermal diffusivity in the scattering object R from that of the surrounding (reference) region R_0. The ratio in equation (12) has been symbolized by $n(\boldsymbol{r})$ deliberately, to suggest the analogy of this parameter to the effects of variations in the refractive index in conventional optical propagating fields. Upon separating out the thermal-wave field into incident and scattered components,

$$T(\boldsymbol{r}) = T_i(\boldsymbol{r}) + T_s(\boldsymbol{r}) \tag{13}$$

and using the free-space Green's function, one obtains [19]

$$T_s(\boldsymbol{r}) = \int_{A_0} \int F(\boldsymbol{r}_0) T(\boldsymbol{r}_0) G_0(\boldsymbol{r}|\boldsymbol{r}_0)\, \mathrm{d}A_0 \qquad \boldsymbol{r} \in (R, S). \tag{14}$$

In equation (14) the integration is performed over the slice A_0 of the spatial object region R enclosed by the boundary line S; $T_s(\boldsymbol{r})$ is assumed to be subject to any appropriate homogeneous Dirichlet or Neumann conditions at the source-coordinate boundary $\boldsymbol{r}_0^s$, and so is the $G_0(\boldsymbol{r}|\boldsymbol{r}_0)$ on both $\boldsymbol{r}_0^s$ and $\boldsymbol{r}^s$ (observation-coordinate) boundaries. If the thermal-wave source point $\boldsymbol{r}_0$, and/or observation point $\boldsymbol{r}$, are not infinitesimally close to the boundary S, then [19]

$$G_0(\boldsymbol{r}|\boldsymbol{r}_0) = G_0(\boldsymbol{r} - \boldsymbol{r}_0). \tag{15}$$

In the case of a weakly scattering field, $|T_s(\boldsymbol{r})| < |T_i(\boldsymbol{r})|$, the first Born approximation to the integral equation (14) can be written:

$$T_s(\boldsymbol{r}) \approx T_B(\boldsymbol{r}) = \int_{A_0} \int F(\boldsymbol{r}_0) T_i(\boldsymbol{r}_0) G_0(\boldsymbol{r} - \boldsymbol{r}_0)\, \mathrm{d}A_0. \tag{16}$$

Upon describing the propagating thermal-wave field in the functional form

$$T(\boldsymbol{r}) = \exp(\psi(\boldsymbol{r})) \qquad \psi(\boldsymbol{r}) = \psi_i(\boldsymbol{r}) + \psi_s(\boldsymbol{r}) \tag{17}$$

so that $T_i(\boldsymbol{r}) = \exp(\psi_i(\boldsymbol{r}))$, the scattered field can be formally expressed in the first Rytov approximation:

$$\psi_s(\boldsymbol{r}) = \frac{1}{T_i(\boldsymbol{r})} \int_{A_0} \int F(\boldsymbol{r}_0) T_i(\boldsymbol{r}_0) G_0(\boldsymbol{r} - \boldsymbol{r}_0)\, \mathrm{d}A_0. \tag{18}$$

Whether in the Born or in the Rytov representation, the validity of the above general three-dimensional considerations to two-dimensional slice theory for diffractive thermal-wave tomographic applications will be assumed to hold if the object space R does not vary rapidly (i.e. it is effectively translationally invariant) within a thermal wavelength in the direction perpendicular to the cross-sectional plane (or set of parallel planes) of interest. A similar assumption has been employed [20] to develop a two-dimensional wave theory for ultrasonic tomographic imaging of material cross-sections [21]. Under these conditions, we approach the photothermal-wave forward tomographic problem in the two-dimensional geometry of figure 1, which corresponds to the pyroelectric detection scheme [9, 11]. The experimental ability to scan both finite size source (laser) and detector (pin probe) apertures renders the geometry of figure 1 qualitatively identical to that used for ultrasonic synthetic aperture diffraction tomography [21], as well as the one used for well-to-well imaging offset vertical seismic profiling in geophysical diffraction tomography [22]. In the context of equation (9), the free-space thermal-wave Green's function in the two spatial dimensions (x, y) of figure 1 is given by

$$(\nabla^2 + \tilde{k}_0^2) G_0(\boldsymbol{r}|\boldsymbol{r}_0) = -\delta(\boldsymbol{r} - \boldsymbol{r}_0). \tag{19}$$

Use can be made of a spatial Laplace transform formulation pertinent to the thermal-wave problem [15],

$$\hat{g}_0(\tilde{\boldsymbol{K}}_s|\boldsymbol{r}_0) = {}^2\mathscr{L}(G_0(\boldsymbol{r}|\boldsymbol{r}_0)) = \int_{A_0} \int G_0(\boldsymbol{r}|\boldsymbol{r}_0) \exp(-\tilde{\boldsymbol{K}}_s \cdot \mathrm{r})\, \mathrm{d}^2\boldsymbol{r} \tag{20}$$

where $\tilde{\boldsymbol{K}}_s$ is the complex spatial wave vector of the scattered thermal-wave field,

$$\tilde{\boldsymbol{K}}_s \equiv 2\pi \tilde{\boldsymbol{f}}_s = \tilde{k}_\alpha \hat{\boldsymbol{i}} + \tilde{k}_\beta \hat{\boldsymbol{j}} \tag{21}$$

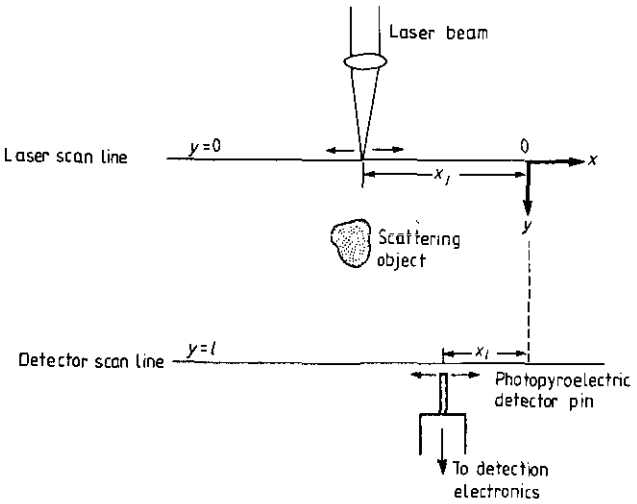

Figure 1. *Geometry for synthetic aperture photothermal-wave diffraction tomography using scanning thin-film pyroelectric detection. The sample thickness l is assumed uniform. The sample surface lies at $y=0$. For each position of the laser beam waist on line $y=0$ (transmitting aperture), the metal pin detector measures the thermal-wavefield characteristics (amplitude and phase) along the back surface $y=l$ line. The thin-film pyroelectric transducer in contact with the sample at $y=l$ is assumed to be of negligible thickness compared to l and thus entirely thermally thin at audio modulation frequencies.*

and $\tilde{f}_s$ is the complex scattered spatial-frequency vector. Upon transformation of equation (19) and use of the vanishing boundary condition for $G_0(r^s|r_0)$, the formal solution for $\hat{g}_0$ is

$$\hat{g}_0(\tilde{K}_s|r_0)=\frac{e^{-\tilde{K}_s\cdot r_0}}{\tilde{K}_s^2-\tilde{k}_0^2}. \tag{22}$$

Inversion of equation (22) requires defining appropriately converging contours in the complex spatial frequency domains ($\tilde{k}_\alpha$, $\tilde{k}_\beta$):

$$G_0(r|r_0)=\frac{1}{4\pi^2}\oint_{C_\alpha}\oint_{C_\beta}\hat{g}_0(\tilde{K}_s|r_0)\,e^{\tilde{K}\cdot r}\,d^2K_s \tag{23}$$

where the contours C_α and C_β remain to be determined. Before proceeding with this task, it is important to realize that the existence of the inverse equation (23) presupposes, and must be consistent with, the existence of a closure relation in the particular complex spatial thermal wavenumber (or frequency) space defined by variables with equal real and imaginary parts. This situation is quite different from the conventional definition of a contour for Laplace inversion integrals [23] where the path of integration is upward along a straight line $\mathrm{Re}(s)=c=$ constant, and c is chosen so that the Laplace transform may be analytic to the right of this line. Generalized Laplace transform inversion contours are required, adapted to the specific properties of the thermal-wave complex Laplace variable vector $\tilde{K}_s$. Many such generalized Laplace inversion contours in one dimension have been previously considered and examined in some detail by Carslaw [24]. In thermal-wave physics the desired closure relation amounts to the proof of existence of the Dirac delta function in the complex spatial frequency domain, as shown in appendix 1.

Equations (22) and (23) yield

$$G_0(\boldsymbol{r}-\boldsymbol{r}_0)=\frac{1}{4\pi^2}\oint_{C_\alpha} \mathrm{d}k_\alpha \oint_{C_\beta} \frac{\exp[\tilde{k}_\alpha(x-x_0)+\tilde{k}_\beta(y-y_0)]}{\tilde{k}_\beta^2-(\tilde{k}_0^2-\tilde{k}_\alpha^2)}\,\mathrm{d}k_\beta. \tag{24}$$

For the integration over k_β let $z=R\,\mathrm{e}^{\mathrm{i}(\Theta+\pi/4)}$. This definition of a complex variable amounts to rotating the contour through an angle $\pi/4$ and guarantees convergence of the new contour, provided that the original unrotated contour exists in the mean-square sense [25]. Detailed conditions for regular behaviour of the integral after the rotation are given by Pólya [26]. From the exponent in equation (24):

$$\mathrm{Re}[(y-y_0)z]=(y-y_0)R\cos\left(\Theta+\frac{\pi}{4}\right). \tag{25}$$

If $y-y_0>0$, then $y-y_0=|y-y_0|$; choosing $\cos(\Theta+\pi/4)<0$, i.e. $\pi/4<\Theta<5\pi/4$, yields an integrand of exponential type and a convergent integral. If $y-y_0<0$, then $-3\pi/4<\Theta<\pi/4$ is the appropriate sector in the complex k_β plane. Here we shall only consider the former condition since we are interested in the forward propagation of photothermal waves along the y-axis of figure 1 (in backward propagation thermal-wave fields become unbounded). We will thus define C_β as shown in figure 2. Applying the theorem of residues to the integral

$$I_\beta \equiv \oint_{C_\beta} \frac{\exp[\tilde{k}_\beta(y-y_0)]}{\tilde{k}_\beta^2-(\tilde{k}_0^2-\tilde{k}_\alpha^2)}\,\mathrm{d}k_\beta \tag{26}$$

with poles at

$$\tilde{k}_\beta^{(\pm)}=\pm(\tilde{k}_0^2-\tilde{k}_\alpha^2)^{1/2}=\pm\tilde{k}_0(1-p_\alpha^2)^{1/2} \tag{27}$$

where

$$p_\alpha \equiv k_\alpha/k_0 \tag{28}$$

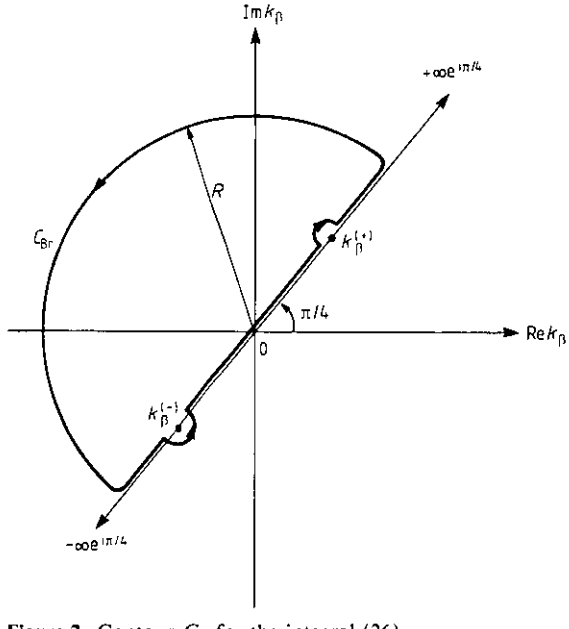

Figure 2. Contour C_β for the integral (26).

we obtain

$$I_\beta = -i\pi \frac{\exp(-\tilde{k}_0|y-y_0|\sqrt{1-p_\alpha^2})}{\tilde{k}_0\sqrt{1-p_\alpha^2}}. \tag{29}$$

The residue at $\tilde{k}_\beta = \tilde{k}_\beta^{(+)}$ has been rejected using the Feynman contour shown in figure 2 along the line $(-\infty\, e^{i\pi/4}, \infty\, e^{i\pi/4})$, as it makes I_β increase without bound for large values of $|\tilde{k}_0|$. Then equation (24) becomes

$$G_0(\boldsymbol{r}-\boldsymbol{r}_0) = -\frac{i\, e^{-i\pi/4}}{4\pi} \oint_{C_\alpha} \frac{\exp\{\tilde{k}_0[(x-x_0)p_\alpha - |y-y_0|\sqrt{1-p_\alpha^2}]\}}{\sqrt{1-p_\alpha^2}}\, dp_\alpha. \tag{30}$$

The contour C_α may be easily determined upon consideration of exponential convergence. Let $p_\alpha = R\, e^{i\Theta}$ and require

$$\lim_{R\to\infty} \{\mathrm{Re}[\tilde{k}_0(x-x_0)R\, e^{i\Theta} - \tilde{k}_0|y-y_0|(1-R^2\, e^{2i\Theta})^{1/2}]\}$$

$$= k_0 R\left[(x-x_0)\cos\left(\Theta+\frac{\pi}{4}\right) - |y-y_0|\sin\left(\Theta+\frac{\pi}{4}\right)\right] \to -\infty. \tag{31}$$

Assuming only the case $x-x_0>0$, the common sector $[\cos(\Theta+\pi/4)<0]\cap[\sin(\Theta+\pi/4)>0] = [\pi/4\leq\Theta\leq 3\pi/4]$ defines the extent of the validity of the integral (30). similar considerations for the case $x-x_0<0$ lead to a contour spanning the common sector $[-\pi/4\leq\Theta\leq\pi/4]$, with results identical to equation (35) below. The contour C_α is shown in figure 3. Taking into account the vanishing of the integral over the Bromwich contour C_{Br} as $R\to\infty$ and carrying out the integration along the line $(-\infty\, e^{-i\pi/4}, 0]$ above the branch cut, we obtain

$$J_0(\boldsymbol{r}-\boldsymbol{r}_0) \equiv -\frac{i}{4\pi} e^{-i\pi/4}\left(\lim_{\substack{\varepsilon\to 0\\ \rho\to 0}} \int_{-\infty}^{0} \frac{f(p_\alpha+i\varepsilon)}{\sqrt{1-(p_\alpha+i\varepsilon)^2}}\, dp_\alpha + \int_C \frac{f(z)}{\sqrt{1-z^2}}\, dz\right)$$

$$= 2\pi i\, \mathrm{Res} \sum_{j=0}^{N} (p_\alpha = z_j) = 0 \tag{32}$$

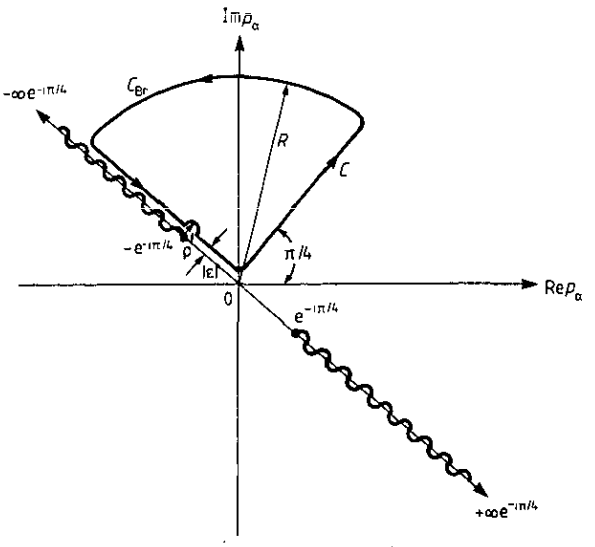

Figure 3. Contour C_α for the integral (30).

where

$$f(z) \equiv \exp[\tilde{k}_0(|x-x_0|z - |y-y_0|\sqrt{1-z^2})]. \tag{33}$$

From equation (33) let

$$G_0(\boldsymbol{r}-\boldsymbol{r}_0) = -\frac{\mathrm{i}}{4\pi}\mathrm{e}^{-\mathrm{i}\pi/4}\int_C \frac{f(z)}{\sqrt{1-z^2}}\,\mathrm{d}z$$

$$= \frac{\mathrm{i}}{4\pi}\mathrm{e}^{-\mathrm{i}\pi/4}P\int_{-\infty}^{0}\frac{\exp[\tilde{k}_0(|x-x_0|p_\alpha - |y-y_0|\sqrt{1-p_\alpha^2})]}{\sqrt{1-p_\alpha^2}}\,\mathrm{d}p_\alpha \tag{34}$$

or

$$G_0(\boldsymbol{r}-\boldsymbol{r}_0) = \frac{\mathrm{i}}{4\pi}\mathrm{e}^{-\mathrm{i}\pi/4}P\int_0^{\infty}\frac{\mathrm{e}^{-\tilde{k}_0|x-x_0|p_\alpha}}{\sqrt{1-p_\alpha^2}}\exp(-\tilde{k}_0|y-y_0|\sqrt{1-p_\alpha^2})\,\mathrm{d}p_\alpha. \tag{35}$$

In appendix 2 we have investigated the contour of validity for integral representation of $G_0(\boldsymbol{r}-\boldsymbol{r}_0)$, and a convenient analytic expression for the integral (35). In the case of a semi-infinite, homogeneous two-dimensional domain R_0, the thermal-wave field due to an aperture function $\alpha_0(x_0, y_0)$ is given by [15]

$$T(x, y) = \int_{A_0}\int \alpha_0(x_0, y_0)G_0(\boldsymbol{r}-\boldsymbol{r}_0)\,\mathrm{d}A_0. \tag{36}$$

For a point-source excitation of strength T_0 at the origin, use of equation (A2.16) yields

$$T(x, y) = T_0\frac{\mathrm{e}^{-\mathrm{i}\pi/4}}{4\pi}\mathscr{K}_0(\tilde{k}_0\sqrt{x^2+y^2}). \tag{37}$$

Furthermore, in terms of Thomson functions [27]

$$\mathscr{K}_0(k_0 r\,\mathrm{e}^{\mathrm{i}\pi/4}) = \mathrm{ker}(k_0 r) + \mathrm{i}\,\mathrm{kei}(k_0 r). \tag{38}$$

Now, thermal-wave field amplitude and phase lag may be explicitly calculated:

$$|T(x, y)| = \frac{T_0}{4\pi}[\mathrm{ker}^2(k_0\sqrt{x^2+y^2}) + \mathrm{kei}^2(k_0\sqrt{x^2+y^2})]^{1/2} \tag{39}$$

and

$$\phi(x, y) = \frac{\pi}{4} + \tan^{-1}\left(\frac{\mathrm{kei}(k_0\sqrt{x^2+y^2})}{\mathrm{ker}(k_0\sqrt{x^2+y^2})}\right). \tag{40}$$

At large distances from the origin, the asymptotic representation [27] for the Kelvin function gives

$$|T(r)| \approx \frac{T_0}{4\sqrt{2\pi}}\frac{\mathrm{e}^{-k_0 r/\sqrt{2}}}{\sqrt{k_0 r}} \tag{41}$$

and

$$\phi(r) \approx \frac{\pi}{8} + \frac{1}{\sqrt{2}}k_0 r \tag{42}$$

as expected [19] for a diffractive propagating field of spherical symmetry generated by a point source.

3. Spatial-frequency domain object-field spectral decomposition

For purposes of concreteness we shall adopt the Born approximation, equation (16), for the description of the thermal-wave scattered field in an inhomogeneous object domain R. The scattering wavevector is given by equation (21). A spectral correlation between $\tilde{\boldsymbol{K}}_s$ and the incident wavevector [15]

$$\tilde{\boldsymbol{k}} = \tilde{k}_x \hat{\boldsymbol{i}} + \tilde{k}_y \hat{\boldsymbol{j}} \equiv 2\pi \tilde{\boldsymbol{f}}_i \tag{43}$$

is possible. First we define the incident spatial frequencies/Laplace variables, given by [15].

$$f_j = j/\lambda_{t0}\sqrt{x^2+y^2} \qquad j = x, y \tag{44}$$

with λ_{t0} representing the thermal wavelength in the incident object region R_0 surrounding the scattering object:

$$\lambda_{t0} = 2\pi(\alpha_0/\omega)^{1/2}. \tag{45}$$

Upon consideration of the Helmholtz-like incident field equation in the geometry of figure 1

$$(\nabla^2 + \tilde{k}_0^2)\, T_i(\boldsymbol{r}) = 0 \tag{46}$$

we proceed with a Laplace transformation along the x-direction. The incident field can be represented by an integral over the relevant spatial frequencies [15], defined over a suitable inversion contour:

$$T_i(\boldsymbol{r}) = \frac{1}{2\pi} \oint_C A(\tilde{k}_x, y)\, e^{\tilde{k}_x x}\, dk_x. \tag{47}$$

Inserting equation (47) into equation (46) yields [15]:

$$A(\tilde{k}_x, y) = A(\tilde{k}_x, 0) \exp(-\tilde{k}_0 y\sqrt{1-p_x^2}) \tag{48}$$

where

$$p_x \equiv k_x/k_0. \tag{49}$$

If, in addition, $T_i(\boldsymbol{r})$ is represented as a propagating plane thermal wave of unit amplitude

$$T_i(\boldsymbol{r}) = \exp(i\tilde{\boldsymbol{k}} \cdot \boldsymbol{r}) \tag{50}$$

then the relationship between the two incident wavevector components can be trivially found from equation (46) to be

$$\tilde{k}_x^2 + \tilde{k}_y^2 = \tilde{k}_0^2 \tag{51}$$

or, in terms of spatial frequencies,

$$f_x^2 + f_y^2 = \lambda_{t0}^{-2}. \tag{52}$$

The inverse of equation (47) may be presented in terms of the bilateral spatial Laplace transform of $T_i(x, y)$:

$$A(\tilde{k}_x, y) = \int_{-\infty}^{\infty} T_i(x, y)\, e^{-\tilde{k}_x x}\, dx. \tag{53}$$

The integral on the right-hand side is meaningful only due to the fact that the spatial frequency f_x changes sign when x changes sign (see equation (44)), thus maintaining the boundedness of the integral. If a different coordinate $-x_t$ is considered along the laser-scanned surface (see figure 1) then it can be easily shown that [21]

$$T_i(x+x_t, y) = \frac{1}{2\pi} \oint_{C_t} A(\tilde{k}_x, y; x_t)\, e^{\tilde{k}_x x}\, dk_x \tag{54}$$

with

$$A(\tilde{k}_x, y; x_t) = A(\tilde{k}_x, y)\, e^{\tilde{k}_x x_t} \tag{55}$$

consistent with the shift theorem of Laplace transformation. This generalized version of the theorem over an arbitrary contour C_t is valid only for well-defined (convergent) contours and use of the Dirac delta distribution (A1.20).

In order to identify a relationship between the spectral decompositions of the incident and scattered thermal wavefields, the coordinate-shifted Born approximation may be written (see equation (16)):

$$T_B(r; \hat{i}x_t) = \int_{A_0} \int F(r_0)\, T_i(r_0 + \hat{i}x_t)\, G_0(r - r_0)\, dA_0. \tag{56}$$

Let the two-dimensional transform of the incident field in scattered field variables be $\hat{T}_i$:

$$\hat{T}_i(\tilde{K}_s; \hat{i}x_t) = {}^2\mathcal{L}(T_i(r_0 + \hat{i}x_t)) = \int_{A_0} \int T_i(r_0 + \hat{i}x_t)\, e^{-\tilde{K}_s \cdot r_0}\, d^2 r_0. \tag{57}$$

Inserting equation (54) in equation (57) and using the corollary to the theorem in appendix 1 we obtain

$$\hat{T}_i(\tilde{K}_s; \hat{i}x_t) = \oint_{C_t} A_0(\tilde{k}_x)\, {}^2\delta(\tilde{K}_s - \tilde{k})\, e^{\tilde{k}_x x_t}\, dk_x \tag{58}$$

where the two-dimensional Dirac delta distribution is defined in terms of a product of distributions:

$${}^2\delta(\tilde{K}_s - k) = {}^2\delta(\tilde{k}_\alpha - \tilde{k}_x, \tilde{k}_\beta - \tilde{k}_y) \equiv \delta(\tilde{k}_\alpha - \tilde{k}_x)\delta(\tilde{k}_\beta - \tilde{k}_y) \tag{59}$$

and

$$A_0(\tilde{k}_x) \equiv A(\tilde{k}_x, y = 0). \tag{60}$$

Further, let the two-dimensional transform of the Born function in scattered field variables be $\hat{T}_B$:

$$\hat{T}_B(\tilde{K}_s; \hat{i}x_t) = {}^2\mathcal{L}(T_B(r; \hat{i}x_t)) \tag{61}$$

and also define

$$\hat{F}(\tilde{K}_s) = {}^2\mathcal{L}(F(r_0)). \tag{62}$$

Equations (56), (61) and (62) yield, in compact form,

$$\begin{aligned} \hat{T}_B(\tilde{K}_s; \hat{i}x_t) &= {}^2\mathcal{L}[(F(r_0)\, T_i(r_0 + \hat{i}x_t))^{**} G_0(r)] \\ &= {}^2\mathcal{L}(F(r_0)\, T_i(r_0 + \hat{i}x_t))^2 (G_0(r)) \end{aligned} \tag{63}$$

where the asterisks indicate two-dimensional spatial convolution. If we define the convolution function

$$\hat{H}(\tilde{\boldsymbol{K}}_s;\ \hat{\imath}x_t) \equiv \hat{F}(\tilde{\boldsymbol{K}}_s)^{**}\hat{T}_i(\tilde{\boldsymbol{K}}_s;\ \hat{\imath}x_t) \tag{64}$$

it is a straightforward matter to show that

$$\hat{H}(\tilde{\boldsymbol{K}}_s;\ \hat{\imath}x_t) = \frac{1}{2\pi}\oint_{C_r} A_0(\tilde{k}_x)\hat{F}(\tilde{\boldsymbol{K}}_s - \tilde{\boldsymbol{k}})\, e^{\tilde{k}\cdot\hat{\imath}x_t}\, dk_x. \tag{65}$$

Now let

$$h(\tilde{\boldsymbol{k}}, \tilde{\boldsymbol{K}}_s) \equiv A_0(\tilde{k}_x)\hat{F}(\tilde{\boldsymbol{K}}_s - \tilde{\boldsymbol{k}}) \tag{66}$$

and regard equation (65) as a Laplace transform in the variable x_t. Inversion yields

$$h(\tilde{\boldsymbol{k}}, \tilde{\boldsymbol{K}}_s) = \int_{-\infty}^{\infty} \hat{H}(\tilde{\boldsymbol{K}}_s;\ \hat{\imath}x_t)\, e^{-\tilde{k}_x x_t}\, dx_t \tag{67}$$

where the bilateral transform can be defined in the sense described earlier. From equations (63) and (64) a relation can be obtained between the transform of the Born field and $\hat{H}$:

$$\hat{T}_B(\tilde{\boldsymbol{K}}_s;\ \hat{\imath}x_t) = (\hat{F}(\tilde{\boldsymbol{K}}_s)^{**}\hat{T}_i(\tilde{\boldsymbol{K}}_s;\ \hat{\imath}x_t))\hat{g}_0(\tilde{\boldsymbol{K}}_s|\boldsymbol{0}) = \hat{H}(\tilde{\boldsymbol{K}}_s;\ \hat{\imath}x_t)/(\tilde{\boldsymbol{K}}_s^2 - \tilde{k}_0^2). \tag{68}$$

Explicitly, from equations (61) and (68),

$$T_B(x, y;\ x_t) = \frac{1}{4\pi^2}\oint_{C_\alpha}\oint_{C_\beta}\left(\frac{\hat{H}(\tilde{k}_\alpha, \tilde{k}_\beta;\ x_t)}{\tilde{k}_\alpha^2 + \tilde{k}_\beta^2 - \tilde{k}_0^2}\right) e^{(\tilde{k}_\alpha x + \tilde{k}_\beta y)}\, dk_\alpha\, dk_\beta. \tag{69}$$

assuming suitable integration contours. For the integration over k_β we are only interested in the values of the scattered field along the detection $y = l$ in figure 1. Consideration of the denominator of the integral over k_β,

$$J_\beta \equiv \oint_{C_\beta}\left(\frac{\hat{H}(\tilde{k}_\alpha, \tilde{k}_\beta;\ x_t)}{\tilde{k}_\beta^2 - (\tilde{k}_0^2 - \tilde{k}_\alpha^2)}\right) e^{\tilde{k}_\beta l}\, dk_\beta \tag{70}$$

with simple poles at $\tilde{k}_\beta^{(\pm)}$ determined by equation (27), gives a relation between the components of the scattered thermal-wavefield wavevector:

$$k_\alpha^2 + k_\beta^2 = k_0^2 \tag{71}$$

or, in terms of the scattered spatial frequencies,

$$f_\alpha^2 + f_\beta^2 = \lambda_{t0}^{-2} = \text{constant}. \tag{72}$$

The appropriate integration contour is that of figure 2, provided that the function $\hat{H}$ is such that Jordan's lemma is satisfied [28]:

$$\lim_{R\to\infty}\left(\frac{|\hat{H}(\tilde{k}_\alpha, R;\ x_t)|}{R^2 - (k_0^2 - k_\alpha^2)}\right) = 0. \tag{73}$$

Retention of the residue at $\tilde{k}_\beta^{(-)}$ only gives

$$J_\beta(\tilde{k}_\alpha;\ x_t) = -i\pi\frac{\hat{J}(\tilde{k}_\alpha, -\tilde{k}_0\sqrt{1-p_\alpha^2};\ x_t)}{\tilde{k}_0\sqrt{1-p_\alpha^2}}\exp(-\tilde{k}_0 l\sqrt{1-p_\alpha^2}). \tag{74}$$

Equation (74) helps reduce the field representation, equation (69), to

$$T_B(x, l;\ x_t) = -\frac{i}{4\pi}\oint_{C_\alpha}\left(\frac{\hat{H}(\tilde{k}_\alpha, -\tilde{k}_0\sqrt{1-p_\alpha^2};\ x_t)}{\tilde{k}_0\sqrt{1-p_\alpha^2}}\exp(-\tilde{k}_0 l\sqrt{1-p_\alpha^2})\right) e^{\tilde{k}_\alpha x}\, dk_\alpha. \tag{75}$$

An important connection between the two-dimensional spatial Laplace transform of the Born field and that of the object (scattering) field $F(r_0)$, equation (62), may now be derived in the form of a Laplace diffraction theorem as shown in appendix 3. The desired two-dimensional scattering object distribution $F(r)$, equation (10), can, in principle, be reconstructed tomographically by its shifted thermal-wave spatial spectral decomposition $\hat{F}(\tilde{K}_s - \tilde{k})$ given by equation (A3.7):

$$\hat{F}(\tilde{f}_\alpha - \tilde{f}_x, \tilde{f}_\beta^{(-)} - \tilde{f}_y) = -\frac{4\pi\, e^{-i\pi/4}}{\lambda_{t0}} \left(\frac{\sqrt{1-(\lambda_{t0} f_\alpha)^2}}{A_0(\tilde{f}_x)} \right) \times \exp\left[2\pi \frac{l}{\lambda_{t0}} e^{i\pi/4} \sqrt{1-(\lambda_{t0} f_\alpha)^2} \right] \hat{t}_B(\tilde{f}_\alpha, \tilde{f}_x). \tag{76}$$

The range of spatial frequencies contained in a tomographic scan in the geometry of figure 1 is determined by the spectral (energy) conservation laws of equation (52) and (72), which consistute a unique relationship between input (x, y) and scattered (α, β) spectra:

$$f_x^2 + f_y^2 = f_\alpha^2 + f_\beta^2 = \lambda_{t0}^{-2} \equiv f_0^2 \qquad f_0(\omega) = \frac{1}{2\pi} (\omega/\alpha)^{1/2}. \tag{77}$$

In view of the form of equation (76) we define spatial frequency combinations [21]

$$f_u \equiv f_\alpha - f_x \tag{78a}$$

$$f_v \equiv f_\beta^{(-)} - f_y = -(f_0^2 - f_\alpha^2)^{1/2} - (f_0^2 - f_x^2)^{1/2}. \tag{78b}$$

It is seen that $f_0 = \lambda_{t0}^{-1}$ is the maximum spatial frequency component contained in the spectral decomposition of the object function, i.e. $|f_\alpha| \leq f_0$ and $|f_x| \leq f_0$. Similar inequalities are satisfied by the dependent frequencies $f_\beta^{(-)}$ and f_y. Now, equations (77) and (78) can be combined to yield the locus of values of f_u, f_v:

$$(f_u + f_x)^2 + (f_v + f_y)^2 = f_0^2 = \text{constant}. \tag{79}$$

This equation shows that, for a given (f_x, f_y) pair of incident frequencies determined by equation (44), all values of the spectral decomposition of the (scattering) object field lie on a circle of radius f_0 centred at the point $(-f_x, -f_y)$ in the spectral (u, v) plane. Figure 4 shows the locus of centres of semicircles containing the range of (f_α, f_β) values which are associated with a particular pair of (f_x, f_y) values and are bounded by the relation $f_\alpha^2 + f_\beta^2 = f_0^2$. The geometrical construction in figure 4 is entirely analogous to those utilized in ultrasonic diffraction tomography [17, 20-22]. Assuming only positive spatial frequencies f_x, f_y and f_u, f_v, it is easy to see that only the upper half-plane contains points corresponding to the scattered thermal-wavefield. These points are bounded by $L_l: (-f_0, 0)$ along the $-f_u$ axis; by $L_r: (f_0, 0)$ along the $+f_u$ axis; and by $L_u: (0, f_0)$ along the $+f_v$ direction. Thus, the spatial frequency content is circumscribed by the two hatched semicircular disks in figure 4. In the field of ultrasonic diffraction tomography the decomposition field of all (f_α, f_β) pairs included in a scanned tomogram was given the name 'coverage' by Nahamoo *et al* [21]. This terminology can be easily adapted within the context of thermal-wave diffraction tomography. It is important to note that as the modulation frequency increases, so does the maximum R_0-domain spatial frequency $f_0(\omega) = \lambda_{t0}^{-1}$, equation (77). This results in enlarged coverage ranges in the (f_u, f_v) space, with an expected resolution enhancement of the reconstructed image. Furthermore, any thermal wavelength decreases are

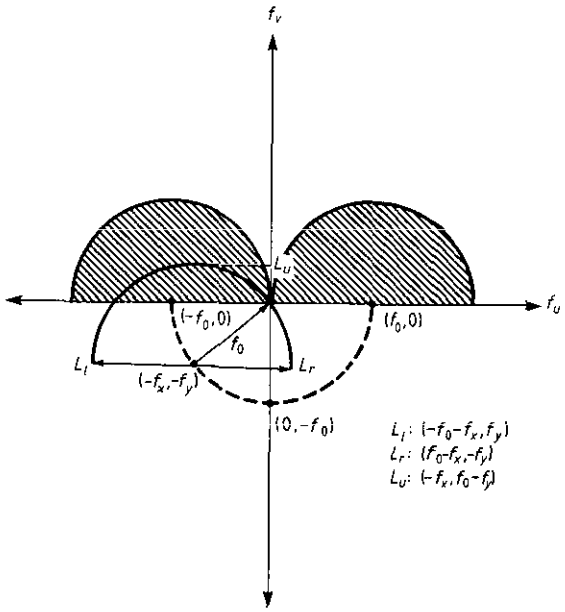

Figure 4. Spectral decomposition loci for thermal-wave scattering spatial frequency content. Each arc is centred at a point $(-f_x, -f_y)$ on a circle defined by equation (77), and it describes equation (79).

expected to lead to a behaviour similar to X-ray propagating fields [17], i.e. a closer resemblance to straight line/ray-optic transmission of thermal waves with substantial decrease in the importance of diffraction. Such ray-like behaviour has been discussed by Burt [29, 30] within the framework of conventional photothermal detection, and has also been of limited experimental success tomographically, as reported elsewhere [11]. In the present context, equation (77) indicates that a modulation frequency increase results in an increase in the arc radius of the scattered field domain in figure 4. This trend is expected to reduce diffraction via the concomitant increase in thermal wavenumber k_0, with an enhancement of ray-like propagation at higher frequencies. True ray-optic behaviour could be expected in the limit of infinite modulation frequency, corresponding to zero wavelength and infinite wavenumber. Experimental support of this discussion in terms of diminishing distortions with increasing frequency in reconstructed tomograms using ray-optic algorithms has already been observed [11]. Appropriate reconstruction methodologies for the scheme of equation (76) and figure 4 using numerical Laplace transforms will be dealt with in a future publication.

4. Conclusions

The mathematical foundations of thermal-wave diffraction tomography have been presented in terms of a two-dimensional spatial Laplace transform formalism based on pseudowave propagation satisfying a diffusive Helmholtz-like equation. The theory led to a Laplace diffraction theorem, linking the transform of the Born approximation (related to the experimentally measured scattered field) to that of the scattering object, over the (primary) scattered and incident complex spatial thermal-wave frequencies. A compact visualization of the magnitude locus of the spectral decomposition of the

scattering object was also presented and shown to be equivalent to that describing propagating wavefields satisfying the proper Helmholtz equation. The present work may be used as the basis for diffractive tomographic reconstructions of the scattering object field via the Laplace diffraction theorem, which offers a powerful method by linking the tomographic image of a cross-sectional scattering object to the two-dimensional Laplace transform inversion of the experimentally measurable thermal-wave signal, modified by the transform of the (experimentally easily determinable) incident aperture. The most severe shortcoming of the present theory impacting experimental situations is expected to be the Born (or Rytov) assumption of weakly scattering fields, needed to validate equations (16) and (18). Extensive discussions of these approximations have been presented elsewhere [17, 20, 21].

Acknowledgments

The author wishes to acknowledge the financial support of the Natural Sciences and Engineering Research Council (NSERC) of Canada and the Ontario Laser and Lightwave Research Center (OLLRC) throughout this work.

Appendix 1

Theorem. In the complex thermal wavenumber domain the Dirac delta function is defined as the limit of the complex distribution

$$e^{i\pi/4} \lim_{\omega\to\infty} P\left(\frac{\sin(\tilde{k}\omega)}{\pi\tilde{k}}\right) = \delta(\tilde{k}) \tag{A1.1}$$

(where P stands for the Cauchy principal value), along the line $(-\infty\, e^{-i\pi/4}, \infty\, e^{-i\pi/4})$ connected by a Bromwich contour in the half-plane $-\pi/4 \leqslant \Theta \leqslant 3\pi/4$.

Proof. Consider the integral

$$J(\omega) = \oint \frac{\exp(i\omega k\, e^{i\pi/4})}{k\, e^{i\pi/4}} f(k)\, dk \tag{A1.2}$$

where $f(k)$ is any analytical function of the complex variable k. Letting, in polar coordinates, $k = R\, e^{i\Theta}$, the contour for converging behaviour of $J(\omega)$ can be determined by

$$\lim_{R\to\infty} \oint_{C_{Br}} \frac{\exp(i\omega R\, e^{i(\Theta+\pi/4)})}{R\, e^{i(\Theta+\pi/4)}} f(R\, e^{i\Theta})\, dR = 0. \tag{A1.3}$$

The real part of the exponent $i\omega r\, e^{i(\Theta+\pi/4)}$ exhibits negative behaviour if, and only if, $\sin(\Theta+\pi/4) > 0$, for values $\omega > 0$. Therefore, a decaying exponential is obtained if $-\pi/4 \leqslant \Theta \leqslant 3\pi/4$, in which case Jordan's lemma gives equation (A1.3) on C_{Br} (figure 5) provided that

$$\lim_{R\to\infty} \left(\frac{f(k)}{k}\right) = 0$$

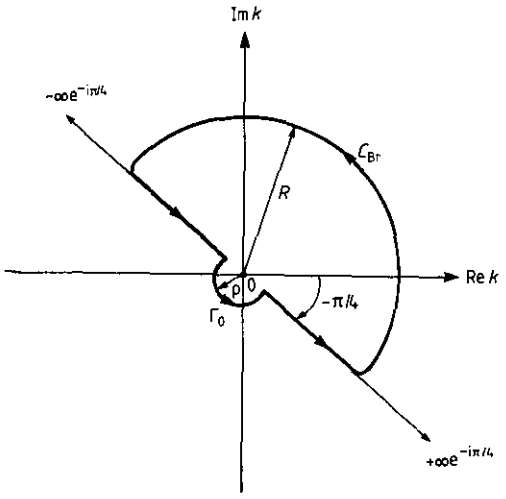

Figure 5. Contour for the integral (A1.2).

and $f(k)$ is bounded. Furthermore, on Γ_0,

$$J_{\Gamma_0}(\omega) = \lim_{\rho\to 0} \oint_{\Gamma_0} \frac{\exp(i\omega k\, e^{i\pi/4})}{k\, e^{i\pi/4}} f(k)\, dk \tag{A1.4}$$

$$= i\, e^{-i\pi/4} \lim_{\rho\to 0} \int_{3\pi/4}^{7\pi/4} \exp(i\omega\rho\, e^{i\Theta+\pi/4)}) f(\rho\, e^{i\Theta})\, d\Theta$$

$$= i\, e^{-i\pi/4} f(0) \lim_{\rho\to 0} \int_{3\pi/4}^{7\pi/4} \exp(-\rho\omega\, e^{i(\Theta-\pi/4)})\, d\Theta \tag{A1.5}$$

where

$$f(0) = \lim_{\rho\to 0} f(\rho\, e^{i\Theta}) \qquad \frac{3\pi}{4} \leqslant \Theta \leqslant \frac{7\pi}{4}. \tag{A1.6}$$

Equation (A1.3) is equivalent to $f(k)$ being regular in $R = [3\pi/4, 7\pi/4]$. Letting $t \equiv \Theta - \pi/4$ and $e^{it} = -i\xi$, we obtain

$$J_{\Gamma_0}(\omega) = e^{-i\pi/4} f(0) \lim_{\rho\to 0} \int_{-1}^{1} \frac{e^{i\omega\rho\xi}}{\xi}\, d\xi \tag{A1.7}$$

and, upon variable redefinition,

$$J_{\Gamma_0}(\omega) = e^{-i\pi/4} f(0) \lim_{\rho\to 0} \int_{-\rho\omega}^{\rho\omega} \frac{e^{ix}}{x}\, dx \tag{A1.8}$$

so that

$$\lim_{\omega\to\infty} J_{\Gamma_0}(\omega) = e^{-i\pi/4} f(0) \left(P \int_{-\infty}^{\infty} \frac{e^{ix}}{x}\, dx \right) = i\pi\, e^{-i\pi/4} f(0). \tag{A1.9}$$

Finally, on the straight line $l: (-\infty\, e^{-i\pi/4}, \infty\, e^{-i\pi/4})$ define

$$J_1(\omega) \equiv \int_{-r}^{-\rho} \frac{\exp(i\omega k\, e^{i\pi/4})}{k\, e^{i\pi/4}} f(k)\, dk \tag{A1.10}$$

$$J_2(\omega) \equiv \int_{\rho}^{r} \frac{\exp(i\omega k\, e^{i\pi/4})}{k\, e^{i\pi/4}} f(k)\, dk \tag{A1.11}$$

so that

$$J_l(\omega) = \lim_{\substack{\rho \to 0 \\ r \to \infty}} (J_1(\omega) + J_2(\omega)) = P \int_{-\infty}^{\infty} \frac{\exp(i\omega k\, e^{i\pi/4})}{k\, e^{i\pi/4}} f(k)\, dk. \tag{A1.12}$$

Now, from the theorem of residues,

$$\lim_{\omega \to \infty} J_l(\omega) = \lim_{\omega \to \infty} \oint \frac{\exp(i\omega k\, e^{i\pi/4})}{k\, e^{i\pi/4}} f(k)\, dk = 2\pi i \lim_{\omega \to \infty} [\mathrm{Res}(k=0)] \tag{A1.13}$$

since the only pole of equation (A1.2) is at the origin. Furthermore,

$$\lim_{\omega \to \infty} [\mathrm{Res}(k=0)] = \lim_{\omega \to \infty} \left(\frac{\exp(i\omega k\, e^{i\pi/4})}{\partial(e^{i\pi/4}k)/\partial k} f(k)|_{k=0} \right) = e^{-i\pi/4} f(0). \tag{A1.14}$$

Collecting terms from equations (A1.3), (A1.9) and (A1.12) into equation (A1.13) yields

$$\lim_{\omega \to \infty} \left(P \int_{-\infty}^{\infty} \frac{\exp(i\omega k\, e^{i\pi/4})}{k} f(k)\, dk \right) = i\pi f(0). \tag{A1.15}$$

We use the generalized complex definition

$$\exp(i\omega z) = \cos(\omega z) + i \sin(\omega z) \qquad z = \tilde{k} \tag{A1.16}$$

and from the (formally) imaginary components of equation (A1.15) we obtain

$$\lim_{\omega \to \infty} \left(P \int_{-\infty}^{\infty} \frac{\sin(\omega \tilde{k})}{\pi k} f(k)\, dk \right) = f(0) \tag{A1.17}$$

where it is understood that only the principal value of the imaginary part of the expression for $\exp\{i[\omega k(1+i)/\sqrt{2}]\}$,

$$\mathrm{Im}[\exp(i\omega k\, e^{i\pi/4})] = \exp(-\omega k/\sqrt{2}) \sin(\omega k/\sqrt{2}) \tag{A1.18}$$

is to be retained under the integral sign on the left-hand side. A comparison of equations (A1.1) and (A1.17) proves the definition of the Dirac delta function distribution† in thermal-wavenumber domain and in the sense of the contour shown in figure 5:

$$\int_{-\infty}^{\infty} \delta(\tilde{k}) f(k)\, dk = f(0). \tag{A1.19}$$

Corollary. An integral representation of the thermal-wavenumber domain Dirac delta function is

$$\delta(\tilde{k}) = \frac{e^{i\pi/4}}{2\pi} P \int_{-\infty}^{\infty} e^{i\omega\tilde{k}}\, d\omega \tag{A1.20}$$

along the line $(-\infty\, e^{-i\pi/4}, \infty\, e^{-i\pi/4})$.

Proof. Let

$$Q(\tilde{k}) \equiv P \int_{-\infty}^{\infty} e^{i\omega\tilde{k}}\, d\omega. \tag{A1.21}$$

† For a proof of the Dirac delta function distribution along the real axis see, for example, [31].

Now

$$Q(\tilde{k}) = \lim_{\omega\to\infty}\left(P\int_{-\omega}^{\omega} e^{i\omega\tilde{k}}\,d\omega\right) \tag{A1.22}$$

$$= \lim_{\omega\to\infty} P\left(\frac{1}{i\tilde{k}} e^{i\omega\tilde{k}}\Big|_{-\omega}^{\omega}\right) = \lim_{\omega\to\infty} P\left(2\frac{\sin(\omega\tilde{k})}{\tilde{k}}\right). \tag{A1.23}$$

Therefore, using the foregoing theorem,

$$Q(\tilde{k}) = 2\,e^{-i\pi/4}\pi\delta(\tilde{k}) \tag{A1.24}$$

and equation (A1.20) follows immediately from equations (A1.21) and (A1.24).

Appendix 2. Integral representation of two-dimensional thermal-wave Green's function for semi-infinite domain

Consider the modified integral of equation (35):

$$J(|x-x_0|, |y-y_0|) = P\int_{-\infty}^{\infty} \frac{e^{-\tilde{k}_0|x-x_0|p_\alpha}}{\sqrt{1-p_\alpha^2}} \exp(-\tilde{k}_0|y-y_0|\sqrt{1-p_\alpha^2})\,dp_\alpha. \tag{A2.1}$$

This integral does not converge in the range $-\infty < p_\alpha < 0$ for all values of $|\tilde{A}|$ and $|\tilde{B}|$, where $\tilde{k}_0|x-x_0| \equiv \tilde{A}$ and $\tilde{k}_0|y-y_0| \equiv \tilde{B}$; however, it will be assumed to be well defined momentarily for purposes of functional form definition of J. The range of convergence will be discussed later. Letting

$$p_\alpha = \sin(\omega - \phi) \qquad \phi = \tan^{-1}(\tilde{B}/\tilde{A}) \tag{A2.2}$$

then, for $p_\alpha \to \pm\infty$, it follows that

$$2ip_\alpha \approx e^{\pm i\omega} \tag{A2.3}$$

or

$$\omega \to \mp i\ln(2p_\alpha) \pm \frac{\pi}{2}. \tag{A2.4}$$

Therefore, equation (A2.1) may be transformed to

$$J(|x-x_0|, y-y_0|) = \int_{i\infty-\pi/2}^{-i\infty+\pi/2} \exp[-\tilde{A}\sin(\omega-\phi) - \tilde{B}\cos(\omega-\phi)]\,d\omega. \tag{A2.5}$$

It is now easy to show that

$$\tilde{A}\sin(\omega-\phi) + \tilde{B}\cos(\omega-\phi) = \tilde{A}[1+(\tilde{B}/\tilde{A})^2]^{1/2}\sin\omega = \tilde{k}_0|\boldsymbol{r}-\boldsymbol{r}_0|\sin\omega \tag{A2.6}$$

A change in the integration variable of equation (A2.5) to $u = i\omega$ yields

$$J(\boldsymbol{r}-\boldsymbol{r}_0) = -i\int_{-\infty-i\pi/2}^{\infty+i\pi/2} \exp(i\tilde{k}_0|\boldsymbol{r}-\boldsymbol{r}_0|\sinh u)\,du. \tag{A2.7}$$

Using the definition of the Hankel function of the first kind [27]:

$$H_v^{(1)}(z) = -\frac{i}{\pi}\int_{-\infty}^{\infty+i\pi} \exp(z\sinh w - vw)\,dw \tag{A2.8}$$

we find formally

$$J(\boldsymbol{r}-\boldsymbol{r}_0) \leftrightarrow \pi H_0^{(1)}(\mathrm{i}\tilde{k}_0|\boldsymbol{r}-\boldsymbol{r}_0|) \tag{A2.9}$$

where the path of integration has yet to be determined.

In exploring the convergence of equation (A2.7), the proper integration contour may be determined by requiring the integrand to be bounded at infinity. Let $u=\eta+\mathrm{i}\xi$:

$$|\exp(\mathrm{i}\tilde{k}_0|\boldsymbol{r}-\boldsymbol{r}_0|\sinh u)| = \exp\left[-\frac{1}{\sqrt{2}}|\boldsymbol{r}-\boldsymbol{r}_0|(\sinh\eta\cos\xi+\cosh\eta\sin\xi)\right]. \tag{A2.10}$$

Equation (A2.10) shows that boundedness is tantamount to

$$\sinh\eta\cos\xi+\cosh\sin\xi>0 \tag{A2.11}$$

or, equivalently,

$$(\cos\xi>0)\cap(\sin\xi>0)\Rightarrow\left[0\leqslant\mathrm{Im}(u)\leqslant\frac{\pi}{2}\right]. \tag{A2.12}$$

Therefore, the appropriate representation of $J(\boldsymbol{r}-\boldsymbol{r}_0)$ consistent with a well-defined integration path is

$$J(\boldsymbol{r}-\boldsymbol{r}_0) = -\mathrm{i}\int_{-\infty}^{\infty+\mathrm{i}\pi/2}\exp(\mathrm{i}\tilde{k}_0|\boldsymbol{r}-\boldsymbol{r}_0|\sinh u)\,\mathrm{d}u \tag{A2.13}$$

or

$$J(\boldsymbol{r}-\boldsymbol{r}_0) = \frac{\pi}{2}\mathscr{H}_0^{(1)}(\mathrm{i}\tilde{k}_0|\boldsymbol{r}-\boldsymbol{r}_0|) \tag{A2.14}$$

where the script notation of the Hankel function is introduced as a reminder of its modified definition along the path shown in figure 6 half the extent up the imaginary axis in the u-plane, compared to the conventional definition [27] of $H_0^{(1)}(z)$. Operationally, the conventional Hankel function $H_0^{(1)}$ divided by 2 is used (equation (A2.14)) to account for this integration path difference. From equations (35) and (A2.14), and the relation [32]

$$H_0^{(1)}(\mathrm{i}z) = -\frac{2\mathrm{i}}{\pi}K_0(z) \tag{A2.15}$$

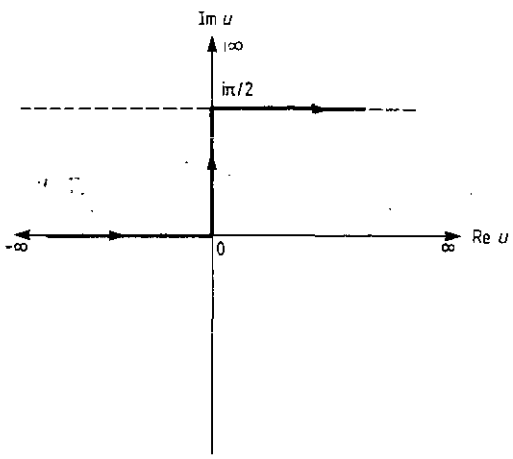

Figure 6. Contour for the integral (A2.14).

where K_0 is the Kelvin function, one obtains

$$G_0(\boldsymbol{r}-\boldsymbol{r}_0)=\frac{e^{-i\pi/4}}{4\pi}\mathscr{K}_0(\tilde{k}_0|\boldsymbol{r}-\boldsymbol{r}_0|). \tag{A2.16}$$

In equation (A2.16) the script notation is, once again, a reminder of the origins of the (modified) definition of the Kelvin function in terms of $\mathscr{K}_0^{(1)}$, rather than $H_0^{(1)}$. It is instructive to note that the conventional zero-order Hankel function of the first kind and of a real argument is obtained in solving the two-dimensional Green's function equation for propagating acoustic waves [21]. In developing the theory of Mirage effect detection of thermal waves in solids, Kuo *et al* [33, 34] obtained a conventional Kelvin-functional dependence of the temperature field along a two-dimensional cross-section defined by a line (the probe laser beam) and the point of incidence of the pump laser beam onto a solid surface. The present analysis indicates that a modified function is required in order for the solution to be well-defined and bounded.

Appendix 3

Theorem. A Laplace diffraction theorem valid for diffusive thermal-wave scattering media may be constructed in a form analogous to the well-known Fourier diffraction theorem for propagating wavefields (e.g. ultrasonic waves [17]).

Proof. Consideration of the expression in parentheses in equation (75) shows that the Laplace transform of the Born field T_B with respect to k_α may be written as

$$\hat{T}_B(\tilde{k}_\alpha; x_l)=-\frac{e^{i\pi/4}}{2k_0}\left(\frac{\hat{H}(\tilde{k}_\alpha, -\tilde{k}_0\sqrt{1-\tilde{p}_\alpha^2}; x_l)}{\sqrt{1-p_\alpha^2}}\right)\exp(-\tilde{k}_0 l\sqrt{1-\tilde{p}_\alpha^2}). \tag{A3.1}$$

Upon substitution of equation (65) into equation (A3.1)

$$\hat{T}_B(\tilde{k}_\alpha; x_l)=-\frac{e^{i\pi/4}}{4\pi k_0}\left(\frac{\exp(-\tilde{k}_0 l\sqrt{1-p_\alpha^2})}{\sqrt{1-p_\alpha^2}}\right)\oint_{C_l} A_0(\tilde{k}_x)$$
$$\times\hat{F}(\tilde{k}_\alpha-\tilde{k}_x, \tilde{k}_\beta^{(-)}-\tilde{k}_y)\,e^{\tilde{k}_x x_l}\,dk_x. \tag{A3.2}$$

Now evaluating the Born field (equation (75)) at a point x_l along the detection line $y=l$ in figure 1, and replacing the integrand of equation (65) with equation (66) in the representation for $\hat{H}$, yields

$$T_B(x_l, l; x_l)=-\frac{e^{i\pi/4}}{8\pi^2 k_0}\oint_{C_\alpha}$$
$$\times dk_\alpha\left(\frac{\exp(-\tilde{k}_0 l\sqrt{1-p_\alpha^2})}{\sqrt{1-p_\alpha^2}}\oint_{C_l} h(\tilde{k}_x, \tilde{k}_y, \tilde{k}_\alpha)\,e^{\tilde{k}_x x_l}\,dk_x\right)e^{\tilde{k}_\alpha x_l} \tag{A3.3}$$

or, rearranging terms,

$$T_B(x_l, l; x_l)=-\frac{e^{i\pi/4}}{8\pi^2 k_0}\oint_{C_\alpha} dk_\alpha\oint_{C_l}\left(\frac{h(\tilde{k}_x, \tilde{k}_y, \tilde{k}_\alpha)}{\sqrt{1-p_\alpha^2}}\exp(-\tilde{k}_0 l\sqrt{1-p_\alpha^2})\right)$$
$$\times\exp(\tilde{k}_x x_r+\tilde{k}_\alpha x_l)\,dk_x. \tag{A3.4}$$

Guided by the combination of exponents in equation (A3.4), the following two-dimensional bilateral Laplace transform definition is convenient:

$$\hat{t}_B(\tilde{k}_\alpha, \tilde{k}_x) \equiv \int_{-\infty}^{\infty} \int T_B(x_l, l; x_t)\, e^{-(\tilde{k}_x x_t + \tilde{k}_\alpha x_l)}\, dx_l\, dx_t. \tag{A3.5}$$

Inspection of the right-hand side of equation (A3.4) readily identifies $\hat{t}_B$ explicitly:

$$\hat{t}_B(\tilde{k}_\alpha, \tilde{k}_x) = -\frac{e^{i\pi/4}}{2k_0}\left(\frac{h(\tilde{k}_x, \tilde{k}_y, \tilde{k}_\alpha)}{\sqrt{1-p_\alpha^2}}\right) \exp(-\tilde{k}_0 l\sqrt{1-p_\alpha^2}). \tag{A3.6}$$

Finally, use of equation (66) gives an expression relating spectrally (i.e. in spatial frequency domain) the two-dimensional Laplace transform of the Born field over the scanned input line and detection line coordinates (x_t, x_l), to the two-dimensional Laplace transform of the object scattering field $F(r_0)$ over the coordinates of the probe region R_0:

$$\hat{t}_B(\tilde{f}_\alpha, \tilde{f}_x) = -\frac{e^{i\pi/4}}{4\pi f_0}\left(\frac{\exp[-2\pi\tilde{f}_0 l\sqrt{1-(f_\alpha/f_0)^2}]}{\sqrt{1-(f_\alpha/f_0)^2}}\right) A_0(\tilde{f}_x)\hat{F}(\tilde{f}_\alpha - \tilde{f}_x, \tilde{f}_\beta^{(-)} - \tilde{f}_y). \tag{A3.7}$$

Equation (A3.7) can be construed to be the desired Laplace diffraction theorem, linking the transform of the (experimentally measurable) scattered thermal-wavefield to the transform of the scatterer to be determined tomographically, modified by the spectral distribution of the incident photothermal aperture A_0, represented by the laser beam waist intensity profile at the material surface of incidence.

References

[1] Busse G 1985 *IEEE Trans. Sonics Ultrasonics* **SU-32** 355
[2] Sawada T, Shimizu H and Oda S 1981 *Japan J. Appl. Phys.* **20** L25
Busse G and Rosencwaig A 1980 *Appl. Phys. Lett.* **36** 815
Arnold W, Hoffman B and Willems H 1986 *Z. Phys.* B **64** 31
[3] Luukkala M 1980 *Scanned Image Microscopy* ed E A Ash (London: Academic) p 273
Faria Jr I F, Ghizoni C C and Miranda L C M 1985 *Appl. Phys. Lett.* **47** 1154
[4] Wong Y H, Thomas R L and Hawkins G F 1978 *Appl. Phys. Lett.* **32** 538
Thomas R L, Pouch J J, Wong Y H, Favro L D, Kuo P K and Rosencwaig A 1980 *J. Appl. Phys.* **51** 1152
[5] Murphy J C and Aamodt L C 1981 *Appl. Phys. Lett.* **38** 196
Fournier D and Boccara A C 1980 *Scanned Image Microscopy* ed E A Ash (London: Academic) p 347
[6] Nordal P E and Kanstad S O 1981 *Scanned Image Microscopy* ed E A Ash (London: Academic) p 331
Busse G 1981 *Opt. Commun.* **36** 441
[7] Busse G and Renk K F 1983 *Appl. Phys. Lett.* **42** 366
Busse G 1983 *J. Physique* **44** C6-471
[8] Mandelis A and Leung K F 1991 *J. Opt. Soc. Am.* A **8** 186
[9] Mieszkowski M and Mandelis A 1990 *J. Opt. Soc. Am.* A 7 552
[10] Fournier D, Lepoutre F and Boccara A C 1983 *J. Physique* **44** C6-479
[11] Mundidasa M and Mandelis A 1991 *J. Opt. Soc. Am.* in press
[12] Vaez Iravani M and Wickramasinghe H K 1985 *J. Appl. Phys.* **58** 122
[13] Favro L D, Kuo P-K and Thomas R L 1987 *Photoacoustic and Thermal Wave Phenomena in Semiconductors* ed A Mandelis (New York: North-Holland) ch 4
[14] Vaez Iravani M and Nikoonahad M 1987 *J. Appl. Phys.* **62** 4065
[15] Mandelis A 1989 *J. Opt. Soc. Am.* A **6** 298
[16] Stark H (ed) 1987 *Image Recovery: Theory and Application* (Orlando, FL: Academic)
[17] Kak A C and Slaney M 1988 *Principles of Computerized Tomographic Imaging* (New York: IEEE Press) ch 4
[18] Carslaw H S and Jaeger J C 1959 *Conduction of Heat in Solids* 2nd edn (Oxford: Clarendon) ch 1

[19] Morse P M and Feshbach H 1953 *Methods of Theoretical Physics* (New York: McGraw-Hill) ch 7
[20] Nahamoo D and Kak A C 1982 *Ultrasonic diffraction Imaging* Report TR-EE 82-20 (West Lafayette, IN: Purdue University) ch 5
[21] Nahamoo D, Pan S X and Kak A C 1984 *IEEE Trans. Sonics Ultrasonics* **SU-31** 218
[22] Devaney A J 1984 *IEEE Trans. Geosci. Remote Sensing* **GE-22** 3
[23] Mathews J and Walker R L 1970 *Mathematical Methods of Physics* 2nd edn (Menlo Park, CA: Benjamin-Cummings) ch 4
[24] Carslaw H S 1921 *Introduction to the Mathematical Theory of the Conduction of Heat in Solids* 2nd edn (New York: MacMillan)
[25] Titchmarsh E C 1948 *Introduction to the Theory of Fourier Integrals* 2nd edn (Oxford: Clarendon) ch 11.7
[26] Pólya G 1929 *Math. Zeitschrift* **29** 549
[27] Watson G N 1958 *A Treatise on the Theory of Bessel Functions* 2nd edn (Cambridge: Cambridge University Press)
[28] Whittaker E T and Watson G N 1948 *A Course in Modern Analysis* (Cambridge: Cambridge University Press)
[29] Burt J A 1983 *J. Physique* C **6** 453
[30] Burt J A 1986 *Can. J. Phys.* **64** 1053
[31] Papoulis A 1962 *The Fourier Integral and its Applications* (New York: McGraw-Hill)
[32] Gradshteyn I S and Ryzhik I M 1980 *Table of Integrals, Series, and Products* (New York: Academic) entry 8.406.1
[33] Kuo P K, Inglehart L J, Sendler E D, Lin M J, Favro L D and Thomas R L 1985 *Rev. Prog. Non-Destructive Evaluation* **4B** 745
[34] Kuo P K, Sendler E D, Favro L D and Thomas R L 1986 *Can. J. Phys.* **64** 1168